



Planar vortices in a Lorentz symmetry breaking environment

E. Mavigno , H. Belich , G. Luchini ^a

Departamento de Física, Universidade Federal do Espírito Santo, Av. Fernando Ferrari, 514, Goiabeiras, Vitória, ES 29060-900, Brazil

Received: 15 May 2024 / Accepted: 5 November 2024
© The Author(s) 2024

Abstract We revisit planar vortex solutions within a model derived from the dimensional reduction of scalar electromagnetism, with a quartic potential incorporating the Carroll–Field–Jackiw term. We explore analytically and numerically the influence of a Lorentz symmetry-breaking constant field on these configurations and our analysis shows how this constant field can produce a new asymptotic behaviour characterised by damped oscillations of the electric and magnetic fields on the edge of the vortices.

1 Introduction

The search for a theory that would clarify the origin of quantum particles found a very satisfactory description with the Weinberg–Salam–Glashow Standard Model (SM) of particles completed in the 1970s [1]. The electroweak unification inspired by the development of superconductivity, and the work of Anderson [2] clarifying the origin of the mass of the gauge field (Anderson–Higgs mechanism) [3] was crowned with the detection of the Higgs boson at the large hadron collider (LHC) in 2013. Despite being able to successfully describe the strong, weak, and electromagnetic interactions, the gravitational interaction remained outside the SM and this motivated the search for an extension of the Anderson–Higgs mechanism through the spontaneous breaking of the gauge symmetry given by a nonscalar field. The direct consequence of this extension is the Lorentz symmetry breaking of the theory [4–6] which was first proposed by Kostelecký and Samuel [7] in the context of String Theory. By taking into account the renormalizability, these proposals were collected as the Standard Model Extension (SME) [8,9] and by relaxing this condition there were several investigations out of SME (nonminimal SME) [10–21]. Moreover, the Lorentz

symmetry breaking effects may play an interesting role in the context of geometric quantum phases [10,15,22–26].

Effective theories in condensed matter that describe planar phenomena such as the Quantum Hall effect discovered in the 1980s [27] have sparked a growing interest in gauge theories. With the discovery of graphene [28], the proposition of insulators and topological superconductors gave a new description of fermions treated by a Dirac equation. Recently, new materials (Weyl semi metals) [29] were discovered, and they are described by effective theories with Violation of Lorentz Symmetry (VSL) similar to those occurring in the SME. With this new panorama, also topological defects with Lorentz breaking background such as vortices have been investigated [13,30–32].

Here we discuss planar vortices in an environment where a possible material background can promote Lorentz Symmetry Violation (LSV). We consider these vortices configurations in a model obtained by dimensional reduction from a scalar electrodynamics with a Carroll–Field–Jackiw term [5] in $3 + 1$ dimensions. In Sect. 2 we discuss how this dimensional reduction is performed and construct the model in $2 + 1$ dimensional space-time with its respective fields and their dynamical equations and we consider an *ansatz* with the adequate symmetries to study the possibility of vortex configurations for the model. In Sect. 3 the asymptotic behaviour of these fields is analysed and we show that for certain combinations of the Lorentz breaking parameters and the coupling constants of the model the fields may oscillate while decaying away from the vortex's core. In Sect. 4 we present full numerical solutions which exhibit this damped oscillation and in Sect. 5 we give some final remarks on this investigation.

^a e-mail: gabriel.luchini@ufes.br (corresponding author)

2 The Maxwell–Chern–Simons–Higgs model via dimensional reduction

The first proposed modification of 4-dimensional electrodynamics leading to a Lorentz symmetry breaking was done by the addition of the so-called Carroll–Field–Jackiw (CFJ) term [5]

$$\mathcal{L}_{\text{CFJ}} = -\frac{1}{4}\epsilon^{\mu\nu\alpha\beta}v_\mu A_\nu F_{\alpha\beta}, \quad (1)$$

to the usual QED lagrangian, with A_μ being the gauge field and $F_{\mu\nu} = \partial_\mu A_\nu - \partial_\nu A_\mu$ the electromagnetic field strength, while v^μ stands for the components of a constant “anisotropy” 4-vector. In particular, for the scalar electrodynamics, such a Lorentz-violating model is defined by the lagrangian

$$\mathcal{L}_{3+1} = -\frac{1}{4}F_{\bar{\mu}\bar{\nu}}F^{\bar{\mu}\bar{\nu}} - \frac{1}{4}\epsilon^{\bar{\mu}\bar{\nu}\bar{\alpha}\bar{\beta}}v_{\bar{\mu}}A_{\bar{\nu}}F_{\bar{\alpha}\bar{\beta}} + \left(D^{\bar{\mu}}\phi\right)^*D_{\bar{\mu}}\phi - \mathcal{U}(|\phi|), \quad \bar{\mu}, \bar{\nu}, \dots = 0, 1, 2, 3 \quad (2)$$

where the complex scalar (Higgs) field ϕ is minimally coupled to the gauge field via the covariant derivative $D_\mu\phi = \partial_\mu\phi - ieA_\mu\phi$, with e the gauge coupling constant and where we consider the Higgs potential to be

$$\mathcal{U}(|\phi|) = \frac{\lambda}{2}\left(|\phi|^2 - a^2\right)^2 \quad (3)$$

where a is a real constant.

When the dimensional reduction is performed by restricting the spatial dimensions to x^1 and x^2 , taking $\partial_3 A_\mu = 0 = \partial_3 \phi$, defining $A^3 = \chi$ a real scalar field and $v^3 = s$ a scalar parameter, the above lagrangian then becomes

$$\mathcal{L}_{2+1} = -\frac{1}{4}F_{\mu\nu}F^{\mu\nu} - \frac{s}{2}\epsilon^{\mu\alpha\beta}A_\mu\partial_\alpha A_\beta + \chi\epsilon^{\mu\alpha\beta}v_\mu\partial_\alpha A_\beta + \left(D^\mu\phi\right)^*D_\mu\phi + \frac{1}{2}\partial_\mu\chi\partial^\mu\chi - e^2\chi^2|\phi|^2 - \mathcal{U}(|\phi|), \quad (4)$$

with $\mu, \nu, \dots = 0, 1, 2$. So, the introduction of the anisotropy field v^μ through the CFJ term preserves the gauge symmetry of the model leading to a Chern–Simons term in 2+1 dimensions, where the electric field is defined as a vector field with components $E_i \equiv F_{0i}$, $i = 1, 2$, while the magnetic field is given by the scalar $B \equiv -\frac{1}{2}\epsilon_{ij}F_{ij}$. We have obtained a Maxwell–Chern–Simons–Higgs model where the gauge and the Higgs fields are non-minimally coupled to a neutral scalar field.

The dynamical equations for the fields A_μ , ϕ and χ read

$$\partial_\mu F^{\mu\nu} = s\epsilon^{\nu\alpha\beta}\partial_\alpha A_\beta - \epsilon^{\nu\alpha\beta}v_\beta\partial_\alpha\chi - J^\nu, \quad (5a)$$

$$(\square + M_A^2)\chi = \epsilon^{\mu\alpha\beta}v_\mu\partial_\alpha A_\beta, \quad (5b)$$

$$D_\mu D^\mu\phi = -e^2\chi^2\phi - \frac{\delta\mathcal{U}(|\phi|)}{\delta\phi^*}. \quad (5c)$$

where we have used $M_A^2 = 2e^2|\phi|^2$ and defined the 4-current $J^\nu = ie(\phi^*D^\nu\phi - \phi(D^\nu\phi)^*)$.

Vortices are localized field configurations characterized by their finite energy

$$\begin{aligned} \mathcal{E} = & \int \left(\frac{1}{2}(E_i E_i + B^2) + (D_0\phi)^* D_0\phi + (D_i\phi)^* D_i\phi \right. \\ & \left. + \frac{1}{2}(\partial_i\chi)^2 + e^2\chi^2|\phi|^2 + \mathcal{U}(|\phi|) \right) d^2x \\ & - \frac{v_0}{2} \int (\epsilon_{ij}A_i\partial_j\chi - \chi B) d^2x \end{aligned} \quad (6)$$

Considering the dimensionless variable $\rho = ear$, with $r = \sqrt{x^i x^i}$, $i = 1, 2$ and using polar coordinates $x^1 = r \cos \theta$, $x^2 = r \sin \theta$ we introduce the *ansätze* for the fields

$$\begin{aligned} \phi &= ag(\rho)e^{iN\theta}, \quad A_0 = aN\omega_0(\rho), \quad A_\rho = 0, \\ A_\theta &= \frac{N}{e}A(\rho), \quad \chi = aN\chi(\rho) \end{aligned} \quad (7)$$

and rewrite the energy functional as

$$\begin{aligned} \mathcal{E} = & 2\pi a^2 \int_0^\infty \left(N^2 \left\{ \frac{1}{2} \left(\omega_0'^2 + \chi'^2 + \frac{A'^2}{\rho^2} \right) \right. \right. \\ & + g^2 \left(\omega_0^2 + \frac{1}{\rho^2}(1-A)^2 + \chi^2 \right) \left. \right\} \\ & \left. + g'^2 + \frac{\xi}{2}(g^2 - 1)^2 + \frac{N^2\eta}{2\rho}(A\chi' - \chi A') \right) \rho d\rho. \end{aligned} \quad (8)$$

The requirement that the energy density must be localised in space defines the values of the profile functions g , ω_0 , A and χ at spatial infinity. The vacua values of ϕ are given by $|\phi| = a$, which makes the potential vanishes, and so, $g \rightarrow 1$ as $\rho \rightarrow \infty$; this leads to the condition $\chi \rightarrow 0$ for the real scalar field and the vanishing of the electromagnetic field in this limit implies that $A \rightarrow 1$ together with $\omega_0 \rightarrow 0$.

The dynamical equations for the model (5a), (5b) and (5c) are then written as the following system of coupled ordinary differential equations for these functions

$$\begin{aligned} g'' + \frac{1}{\rho}g' - \xi(g^2 - 1)g \\ + N^2g\left(\omega_0^2 - \chi^2 - \frac{1}{\rho^2}(1-A)^2\right) = 0, \end{aligned} \quad (9a)$$

$$A'' - \frac{1}{\rho}A' + 2g^2(1-A) + \rho(\xi\omega_0' - \eta\chi') = 0, \quad (9b)$$

$$\omega_0'' + \frac{1}{\rho}\omega_0' - 2g^2\omega_0 + \frac{1}{\rho}(\xi A' - \mu\chi') = 0, \quad (9c)$$

$$\chi'' + \frac{1}{\rho}\chi' - 2g^2\chi + \frac{1}{\rho}(\eta A' - \mu\omega_0') = 0, \quad (9d)$$

with the dimensionless parameters (notice that the radial component of the anisotropy vector does not play any role in

the dynamics)

$$\eta = \frac{v_0}{ea}, \quad \mu = \frac{v_\theta}{ea}, \quad \zeta = \frac{s}{ea}, \quad \xi = \frac{\lambda}{e^2}. \quad (10)$$

3 Asymptotic behaviour

The set of coupled equations for the profile functions can be solved numerically as we shall discuss later. In this section we consider the behaviour of these functions at spatial infinity where their values are close to their vacuum values. With the substitution

$$g = 1 - H \quad A = 1 - G \quad \omega_0 = -W \quad \chi = -X \quad (11)$$

the system of equations for the profile functions can be linearized to give

$$H'' + \frac{1}{\rho} H' - 2\xi H = 0, \quad (12a)$$

$$G'' - \frac{1}{\rho} G' - 2G + \zeta \rho W' - \eta \rho X' = 0, \quad (12b)$$

$$W'' + \frac{1}{\rho} W' - 2W + \frac{\zeta}{\rho} G' - \frac{\mu}{\rho} X' = 0, \quad (12c)$$

$$X'' + \frac{1}{\rho} X' - 2X + \frac{\eta}{\rho} G' - \frac{\mu}{\rho} W' = 0. \quad (12d)$$

and also defining $G = \rho f(\rho)$, and $\rho_H = \sqrt{2\xi} \rho$, we get

$$\rho_H^2 H'' + \rho_H H' - \rho_H^2 H = 0, \quad (13a)$$

$$\rho^2 f'' + \rho f' - (2\rho^2 - 1) f + \rho^2 (\zeta W' - \eta X') = 0, \quad (13b)$$

$$\rho^2 W'' + \rho W' - 2\rho^2 W + \zeta \rho (\rho f' + f) - \mu \rho X' = 0, \quad (13c)$$

$$\rho^2 X'' + \rho X' - 2\rho^2 X + \eta \rho (\rho f' + f) - \mu \rho W' = 0. \quad (13d)$$

In this approximation we find that the Eq. (13a) can be solved by a modified Bessel function,

$$H = \sqrt{\frac{\pi}{2\rho_H}} e^{-\rho_H} = \sqrt{\frac{\pi}{2\rho\sqrt{2\xi}}} e^{-\sqrt{2\xi}\rho}. \quad (14)$$

For the remaining equations, considering only the relevant terms in the limit of $\rho \rightarrow \infty$, we have

$$f'' - 2f + \zeta W' - \eta X' = 0, \quad (15a)$$

$$W'' - 2W + \zeta f' = 0, \quad (15b)$$

$$X'' - 2X + \eta f' = 0, \quad (15c)$$

and writing

$$f(\rho) = \overline{G} e^{k_G \rho}, \quad W(\rho) = \overline{W} e^{k_W \rho}, \quad X(\rho) = \overline{X} e^{k_X \rho}, \quad (16)$$

we end up with the following algebraic relation for the constants

$$\overline{G} = \frac{\sqrt{\xi^2 - \eta^2}}{\zeta} \overline{W} = \frac{\sqrt{\xi^2 - \eta^2}}{\eta} \overline{X}, \quad (17a)$$

$$k_G = k_W = k_X = -\frac{\sqrt{\xi^2 - \eta^2} + \sqrt{\xi^2 - \eta^2 + 8}}{2}. \quad (17b)$$

where the signs are chosen in order to guarantee the expected decay of the functions. The solutions are then

$$G(\rho) = \overline{G} \rho e^{-\frac{\sqrt{\xi^2 - \eta^2} + \sqrt{\xi^2 - \eta^2 + 8}}{2} \rho}, \quad (18a)$$

$$W(\rho) = \overline{W} e^{-\frac{\sqrt{\xi^2 - \eta^2} + \sqrt{\xi^2 - \eta^2 + 8}}{2} \rho}, \quad (18b)$$

$$X(\rho) = \overline{X} e^{-\frac{\sqrt{\xi^2 - \eta^2} + \sqrt{\xi^2 - \eta^2 + 8}}{2} \rho}, \quad (18c)$$

and the asymptotic profiles of the fields are

$$g = 1 - \sqrt{\frac{\pi}{2\rho\sqrt{2\xi}}} e^{-\sqrt{2\xi}\rho} \quad (19)$$

$$A = 1 - \overline{G} \rho e^{-\frac{\sqrt{\xi^2 - \eta^2} + \sqrt{\xi^2 - \eta^2 + 8}}{2} \rho} \quad (20)$$

$$\omega_0 = -\overline{W} e^{-\frac{\sqrt{\xi^2 - \eta^2} + \sqrt{\xi^2 - \eta^2 + 8}}{2} \rho} \quad (21)$$

$$\chi = -\overline{X} e^{-\frac{\sqrt{\xi^2 - \eta^2} + \sqrt{\xi^2 - \eta^2 + 8}}{2} \rho}. \quad (22)$$

There are three possible types of asymptotic solution depending on the values of the parameters ζ and η in the combination $\Delta \equiv \xi^2 - \eta^2$. For $\Delta \geq 0$ the functions will decay exponentially, but for $-8 < \Delta < 0$ the solutions oscillate with a damping and for $\Delta \leq -8$ the solution is oscillatory. For this last case, in particular, since G , W and X go to zero at spatial infinity, not all configurations with $\Delta < 0$ will be acceptable.

4 Numerical support

The presence of an anisotropic background may affect the behaviour of the fields at the border of the vortices and our asymptotic analysis showed the existence of some limits for the values of the parameter v^0 such that the structure of this configuration remains preserved.

In order to find the numerical solutions of the model we consider a lattice of 1025 points regularly distributed along the interval $0 \leq \rho \leq 64$ and we use the gradient flow method to solve the system of coupled Eqs. (9a), (9b), (9c) and (9d). The boundary conditions for the profile functions at spatial infinity are given by the requirement of finite energy, which was discussed in Sect. 2, and the conditions at the origin are

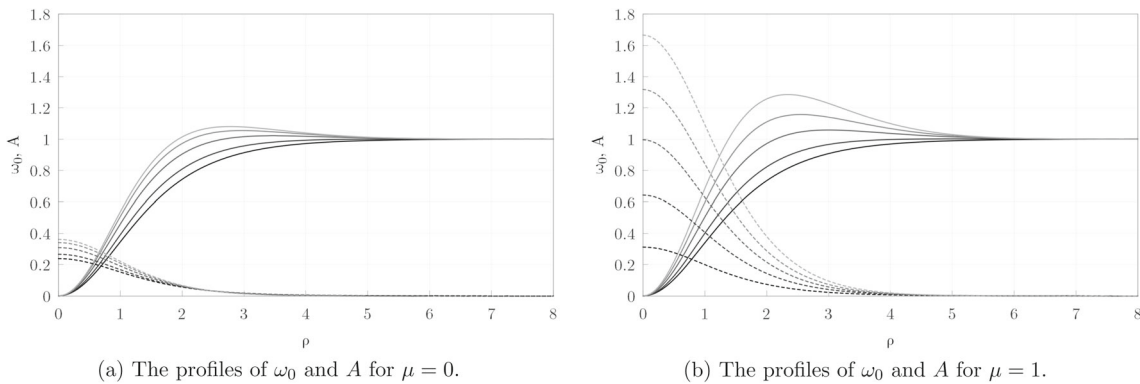


Fig. 1 The solutions for A (solid line) and ω (dashed line) with $\zeta = 0.5$, $\xi = 1$ and $N = 1$ with two different values of μ . The lighter the colour of the curve the greater is the value of η in the range $\eta = 0.0, 0.75, 1.1, 1.25$ and 1.32

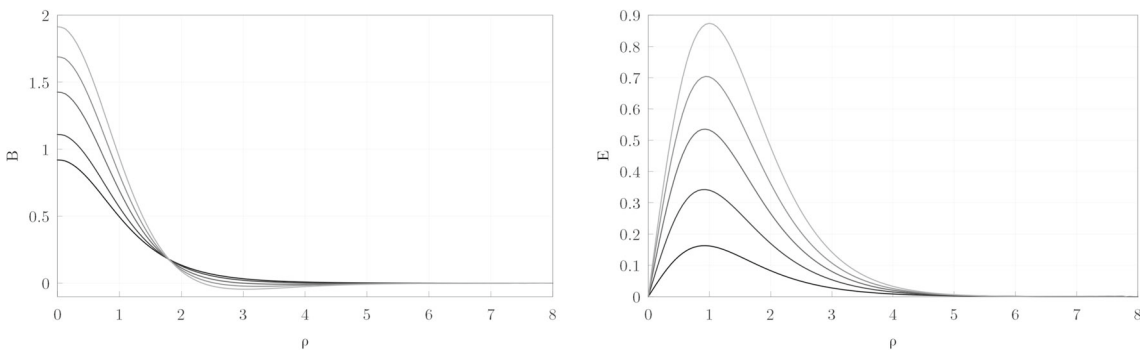


Fig. 2 The profiles of the magnetic and electric fields for $\mu = 1$ and $\eta = 0.0, 0.75, 1.1, 1.25$ and 1.32

obtained directly from the analysis of the differential equations in the limit $\rho \rightarrow 0$: $g = 0$, $A = 0$, $\omega'_0 \rightarrow 0$ and $\chi' \rightarrow 0$.

We are particularly interested in solutions which exhibit a damped oscillatory behaviour for some of the fields far from the vortex core. In the Fig. 1a, b we present the solutions for the profile functions $A(\rho)$ and $\omega_0(\rho)$ for different values of η , keeping all other parameters fixed. In fact, in the whole discussion that follows we consider $N = 1$, $\xi = 1$, $\zeta = 0.5$. We see that for some values of η for which $\Delta < 0$, the behaviour of the solution is such that as η (v_0) increases, starting from the center of the vortex core, the functions will grow faster and eventually oscillate with a damping around their vacuum values, as predicted by the asymptotic analysis. For even greater values of η the solution starts to oscillate without damping and the vortex configuration is lost. The difference between the two solutions depicted in Fig. 1a, b is given by the values of μ , the tangent component of the anisotropy vector. We see that for $\mu \neq 0$ (Fig. 1b), the values of the functions ω_0 and A close to the vortex's core are greater than those for the solutions with $\mu = 0$ (Fig. 1a). We notice that ω_0 is nonzero either when $\zeta \neq 0$ with $\eta = \mu = 0$ or when $\eta \neq 0$ and $\mu \neq 0$ with $\eta = 0$.

Following our *ansatz*, the electric and magnetic fields are respectively a radial vector with component

$$E(\rho) = -N\omega'_0(\rho) \quad (23)$$

and a scalar given by

$$B(\rho) = \frac{N}{\rho} A'(\rho). \quad (24)$$

In Fig. 2 we show the profiles of the electric and magnetic fields for different values of η with $\mu = 0$. The effect of the v^0 component of the anisotropy vector is to produce a damped oscillation in the fields far from the origin when $\Delta < 0$ and this can be better appreciated in Fig. 5 where we have enhanced the points ρ where the electric and magnetic fields change sign; their values are given in Table 1 (Fig. 3).

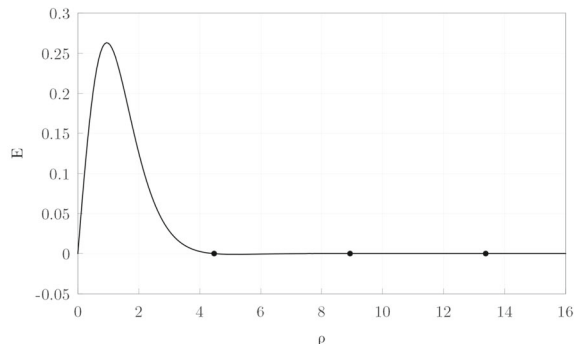
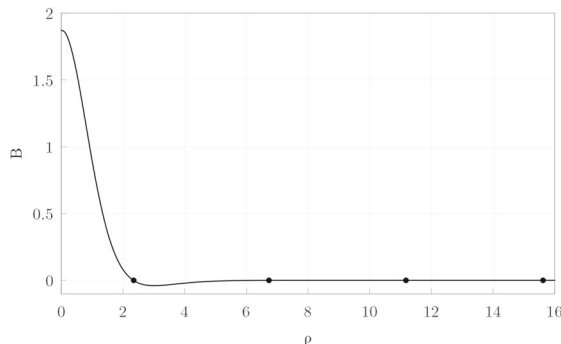
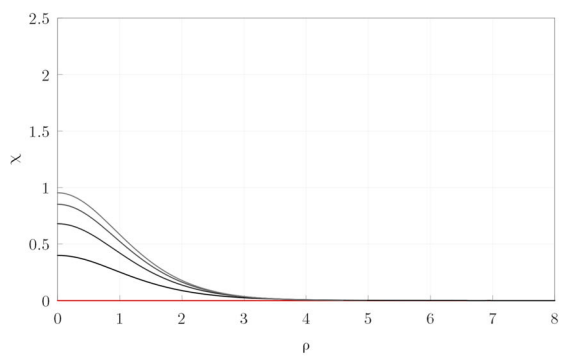
The solutions for the profile of the neutral scalar field are presented in Fig. 4. If $\zeta = \mu = 0$ then, for a nonzero configuration it is required that $\eta \neq 0$; If $\eta = 0$ then a nonzero solution demands $\zeta \neq 0$ and $\mu \neq 0$. In the case we have no background anisotropy, then the neutral field is also zero.

Finally, the energy density function shows that at $\mu = 0$, the energy of the vortex increases alongside the value of η , and its width also expands, as illustrated in Fig. 5a. When the tangential component of the anisotropy vector is nonzero, an

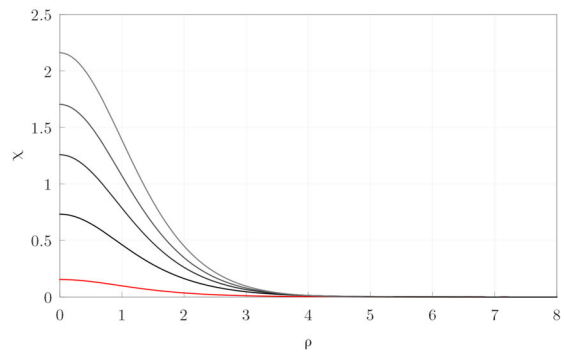
Table 1 Values of ρ where the magnetic and electric fields change sign

$B(\rho)$	$E(\rho)$
2.3440273651921344	4.4676909657123085
6.734473784564999	8.92697209109877
11.173972362784362	13.375864887848005
15.61519822172264	17.822202550190518
20.05684513935638	22.26521048279338
24.49796850947826	26.638516819584922

interesting phenomenon occurs at higher values of the parameter η : for positive μ , the energy density does not peak at the vortex's core; instead, it reaches a peak at an intermediate distance between the origin and the edge of the vortex, and then gradually declines to zero; for negative μ , the energy density peaks at smaller values at the origin.

**Fig. 3** The oscillatory behaviour of the magnetic and electric fields profiles can be observed as these functions change sign as $\rho \rightarrow \infty$ 

(a) The profile of the neutral scalar field for $\mu = 0$. In red, the (trivial) solution for when the background anisotropy vector vanishes.



(b) The profile of the neutral scalar field for $\mu = 1$.

Fig. 4 The profiles for the neutral scalar field are shown for $\mu = 0$ on the left and for $\mu = 1$ on the right. For each case we considered $\eta = 0.0, 0.75, 1.1, 1.25$ and 1.32 . The lighter the color of the curve, the greater is the value of η . The red color specifically depicts the function for which $\eta = 0$

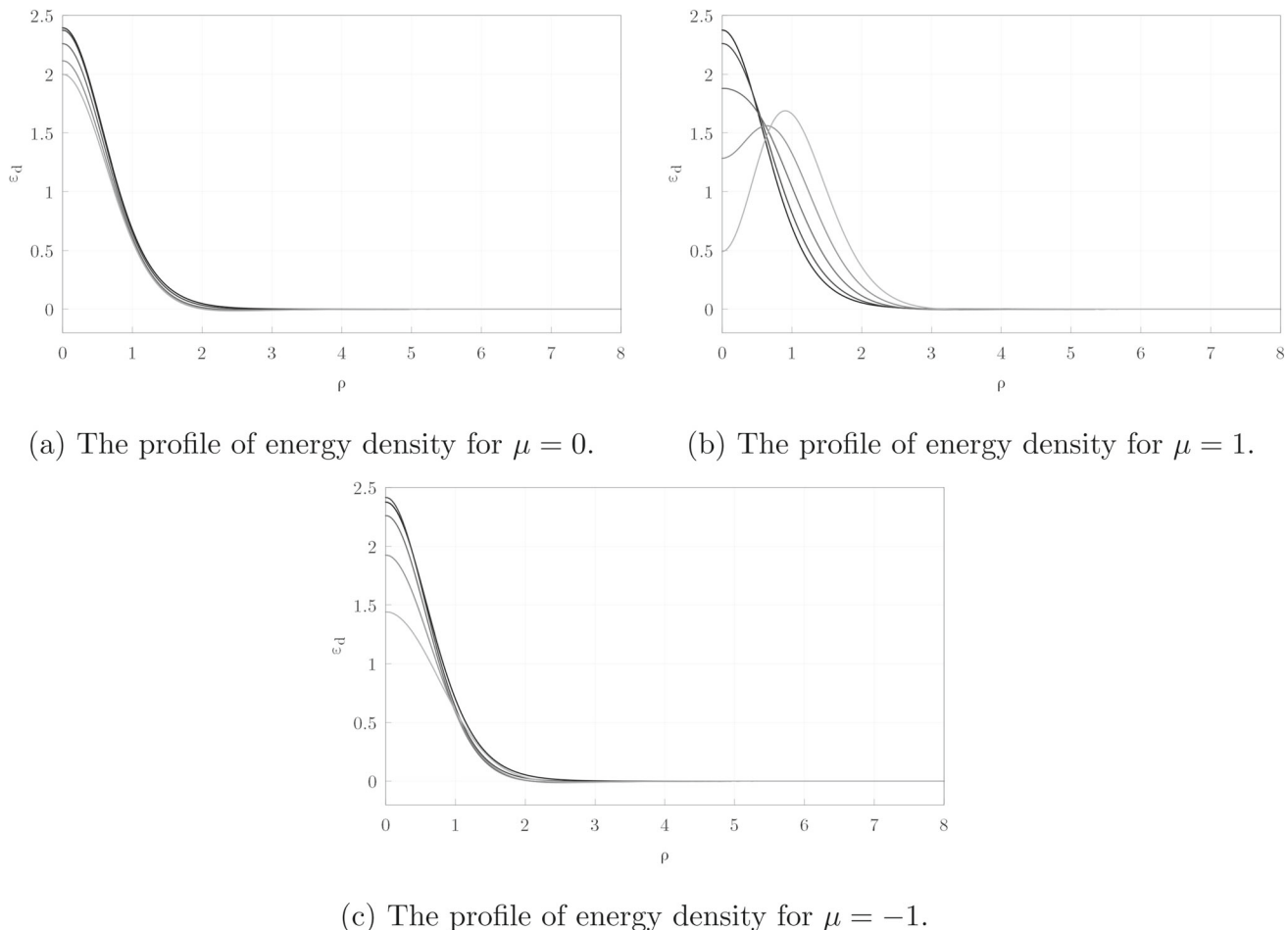


Fig. 5 The energy density profiles are shown for $\mu = 0$ on the left and for $\mu = 1$ on the right and $\mu = -1$ at the bottom. For each case we took values of $\eta = 0.0, 0.75, 1.1, 1.25$ and 1.32

tion, a new neutral scalar field emerges in $2 + 1$ dimensions, and the CFJ term gives rise to a Chern–Simons term, resulting in electrically charged vortices solutions of the dynamical equations for the planar model that we have numerically obtained, as predicted in [13].

Through asymptotic analysis, we discerned how the presence of background anisotropy can influence the behavior of electric and magnetic fields far from the vortex's core. Particularly, when the zeroth component of the background field surpasses the Chern–Simons coupling constant, these fields undergo damped oscillations, a phenomenon confirmed by numerical solutions.

This electric and magnetic flux inversion was previously observed, for instance in [33], for the case of a BPS vortex solution of a Maxwell–Higgs model with a parity-odd Lorentz-violating structure of the CPT-even gauge sector of the SME and a fourth order potential without the Chern–Simons term. Here this phenomenon is also observed for both magnetic and electric fields in a non-BPS regime of a CFJ supplemented Maxwell–Higgs model, suggesting that

this oscillatory damping of the fields may be a robust consequence of Lorentz symmetry violation in vortices across broader scenarios.

The tangential component of the anisotropy field alters the values of the gauge field and the neutral scalar field within the vortex's core. For certain values of η with $\mu \neq 0$, the typical lump-shaped energy density function transforms into one with a local minimum at the vortex's core and a peak at an intermediate distance from the core to the vortex's edge, as it declines to zero. This behaviour may indicate some change in the stability of the solutions [34] due to the increase of the space-time anisotropy.

Acknowledgements H. Belich would like to thank CNPq for financial support.

Data Availability Statement My manuscript has no associated data. [Authors' comment: Data sharing not applicable to this article as no datasets were generated or analysed during the current study.]

Code Availability Statement My manuscript has no associated code/software. [Authors' comment: Code/Software sharing not applicable to

this article as no code/software was generated or analysed during the current study.]

Open Access This article is licensed under a Creative Commons Attribution 4.0 International License, which permits use, sharing, adaptation, distribution and reproduction in any medium or format, as long as you give appropriate credit to the original author(s) and the source, provide a link to the Creative Commons licence, and indicate if changes were made. The images or other third party material in this article are included in the article's Creative Commons licence, unless indicated otherwise in a credit line to the material. If material is not included in the article's Creative Commons licence and your intended use is not permitted by statutory regulation or exceeds the permitted use, you will need to obtain permission directly from the copyright holder. To view a copy of this licence, visit <http://creativecommons.org/licenses/by/4.0/>.

Funded by SCOAP³.

References

1. A. Salam, A. Ali, C. Isham T. Kibble, *Selected Papers of Abdus Salam: (Series on 20th Century Physics)* (World Scientific, 1994)
2. P.W. Anderson, Phys. Rev. **130**, 439 (1963)
3. P.W. Higgs, Phys. Rev. Lett. **13**, 508 (1964)
4. H. Belich, T. Costa-Soares, M.A. Santos, M.T.D. Orlando, Rev. Bras. Ens. Fis. **29**, 1 (2007)
5. S.M. Carroll, G.B. Field, R. Jackiw, Phys. Rev. D **41**, 1231 (1990)
6. V.A. Kostelecký, C.D. Lane, J. Math. Phys. **40**, 6245 (1999)
7. V.A. Kostelecký, S. Samuel, Phys. Rev. D **39**, 683 (1989)
8. D. Colladay, V.A. Kostelecký, Phys. Rev. D **55**, 6760 (1997)
9. D. Colladay, V.A. Kostelecký, Phys. Rev. D **58**, 116002 (1998)
10. H. Belich et al., Eur. Phys. J. C **41**, 421 (2005)
11. H. Belich et al., Phys. Lett. B **639**, 675 (2006)
12. H. Belich et al., Phys. Rev. D **74**, 065009 (2006)
13. H. Belich et al., Int. J. Theor. Phys. **21**, 2415 (2006)
14. H. Belich et al., Phys. Lett. A **370**, 126 (2007)
15. H. Belich et al., Eur. Phys. J. C **62**, 425 (2009)
16. V.A. Kostelecký, M. Mewes, Phys. Rev. D **80**, 015020 (2009)
17. V.A. Kostelecký, M. Mewes, Phys. Rev. D **85**, 096005 (2012)
18. V.A. Kostelecký, M. Mewes, Phys. Rev. D **88**, 096006 (2013)
19. V.A. Kostelecký, Y. Ding, Phys. Rev. D **94**, 056008 (2016)
20. V.A. Kostelecký, Z. Li, Phys. Rev. D **99**, 056016 (2019)
21. V.A. Kostelecký, Z. Li, Phys. Rev. D **103**, 024059 (2021)
22. E.O. Silva, F.M. Andrade, EPL **101**, 51005 (2013)
23. L.R. Ribeiro et al., Int. J. Mod. Phys. A **30**, 1550072 (2015)
24. H. Belich et al., Phys. Rev. D **83**, 125025 (2011)
25. K. Bakke, H. Belich, J. Phys. G Nucl. Part. Phys. **40**, 065002 (2013)
26. K. Bakke, E.O. Silva, H. Belich, J. Phys. G Nucl. Part. Phys. **39**, 055004 (2012)
27. T.H. Hansson, Quantum Hall physics: hierarchies and conformal field theory techniques. Rev. Mod. Phys. **89**, 25005 (2017)
28. A.K. Geim, K.S. Novoselov, Nat. Mater. **6**, 183 (2007)
29. J. Behrends, S. Roy, M.H. Kolodrubetz, J.H. Bardarson, A.G. Grushin, Phys. Rev. B **99**, 140201 (2019)
30. R. Casana, M.M. Ferreira Jr., E. da Hora, A.B.F. Neves, Eur. Phys. J. C **74**, 3064 (2014)
31. R. Casana, G. Lazar, Phys. Rev. D **90**, 065007 (2014)
32. D. Bazeia, R. Casana, M.M. Ferreira Jr., E. da Hora, EPL **109**, 21001 (2015)
33. R. Casana, M.M. Ferreira Jr., E. da Hora, C. Miller, Phys. Lett. B **718**, 620 (2012)
34. C. Herdeiro, E. Radu, E. dos Santos Costa Filho, JCAP **07**, 081 (2024)